



Cite this: DOI: 10.1039/d6an00031b

High- and low-field NMR in binary solvent gradients

Haider Hussain, ^a Paulina Putko, ^b Dariusz Gołowicz, ^c Krzysztof Kazimierzczuk ^{*b} and Matthew Wallace ^{*a}

We introduce composition gradients of the solvent as a powerful new dimension for NMR analysis on both high-field and benchtop instruments. Taking advantage of the differences in the density and miscibility of binary solvent mixtures with different compositions, we layer two solutions at opposite extremes of the compositional range in an NMR tube. The diffusion of the layers into each other establishes a continuous variation in the solvent composition across the sample. Spatially resolved analysis of the sample using either chemical shift imaging (CSI) on high-field NMR instruments or physical movement of the sample (benchtop instruments) enables analysis of chemical systems as a function of the solvent composition. In high field, we determine the pK_a of poorly water-soluble active pharmaceutical ingredients (APIs) in a wide range of compositions of dimethylsulfoxide (DMSO)/water and perform accurate extrapolations to aqueous pK_a using the Yasuda-Shedlovsky method. We thus condense hours of tedious experiments, where the pK_a would be determined separately at each solvent composition, into a single 20 minute experiment. We can also detect the minimum quantity of DMSO required to maintain an API in the freely dissolved state. On a benchtop instrument, we demonstrate how our approach enables the transfer of resonance assignments between spectra of the same compound (asarone) acquired in different solvents (methanol and DMSO). We also show that the method can boost the spectral resolution of complex molecular mixtures (naproxen tablet) *via* the differential solubility of the components in the two solvents.

Received 11th January 2026,
Accepted 20th March 2026

DOI: 10.1039/d6an00031b

rsc.li/analyst

1 Introduction

The solvent in which a chemical system is present is a fundamental component that must be considered to understand the dynamics and kinetics of many chemical systems.¹ A solvent is commonly understood as a part of a solution containing multiple components, where for convenience, one of the components is treated separately and labeled as the solvent. The solvent itself may be a mixture of compounds; nevertheless, the whole mixture can be treated separately from the other components and be labeled a solvent and the rest as solutes.^{2,3}

From the definition of what a solvent is alone one can grasp the relative importance of it with respect to the chemical systems present within it given that the solvent is typically the chemical present in the highest quantity, surrounds all solutes in a way that maximizes solvent-solute interactions, and is the medium in which the solutes “swim”. The solvent thus

impacts all the exchange dynamics that occur between the different solutes, such as molecular diffusion, ion transport, and heat transport to and from chemical reactions.^{2,4,5} These properties have a significant impact on the solubility, stability and reaction rates of chemical systems.^{6–11}

Many studies have been conducted to determine the impact of solvent effects on critical parameters such as pK_a , ion binding and dissolution.^{12,13} These studies generally use a binary solvent mixture where the solvent composition is changed. The effect that this change has on the parameter of interest is measured. For example, potentiometric titrations of pharmaceutically relevant compounds in DMSO/H₂O solution mixtures have been performed to determine the aqueous pK_a of compounds that are too insoluble in water for them to be measured directly.¹⁴ Additionally, solvent effects are used for distinguishing chemical compounds *via* the differing reactions of these compounds to changes in solvent composition.^{15–18} However, a limitation of these approaches is the need for successive manual alteration of the solvent composition, which can have a significant time and material cost associated with it.

In this paper, we present a method of establishing a gradient in solvent composition across the NMR tube due to solvent diffusion. Multiple spatially resolved NMR spectra are then obtained, which enable chemical systems to be analysed as a

^aSchool of Chemistry, Pharmacy and Pharmacology, University of East Anglia, Norwich Research Park, Norwich, NR4 7TJ, UK. E-mail: Matthew.Wallace@uea.ac.uk

^bCentre of New Technologies, University of Warsaw, Banacha 2C, Warsaw, 02-097, Poland. E-mail: k.kazimierzczuk@cent.uw.edu.pl

^cInstitute of Physical Chemistry, Polish Academy of Sciences, Kasprzaka 44/52, Warsaw, 01-224, Poland



function of solvent composition in a “single-shot” NMR experiment. This approach is implemented in a high-field spectrometer to determine the aqueous pK_a of water-insoluble compounds in a 20 minute NMR experiment. A similar approach, exploiting the vertical shift of a sample, is also implemented in two exemplar applications on benchtop instruments. In the first, the resonance assignments of asarone are transferred between methanol and DMSO. In the second, the complex mixtures are resolved *via* the difference in solubility of the different components of the mixture in the two solvents. Continued advances in the resolution and sensitivity of benchtop instruments, along with the provision of pulsed field gradient coils along the vertical axis of the sample tube, may enable the high-field experiments to be implemented on benchtop spectrometers.

2 Methods

2.1 Materials

All chemicals were purchased from Fisher Scientific or Sigma-Aldrich and used as received. Commercially available naproxen tablets were manufactured by Aflofarm Farmacja Polska Sp. z o.o. (Poland).

2,2-Dimethyl-2-silapentane-5-sulfonate (DSS) was the chemical shift reference used in all experiments at high-field. The proton transfer indicators used to determine pK_a as a function of solvent composition were 1,2,4-triazole, sodium formate, sodium acetate, 2-methylimidazole and sodium glycolate. Sodium methanesulfonate (NaMSA) was used as a solvent composition indicator. Stocks of these indicators in 20% H₂O and 80% DMSO-d₆, 80% H₂O and 20% DMSO-d₆ fractional volume (f) were prepared and used throughout the study. The analytes studied at high-field were naproxen, indomethacin, furosemide, quinine hydrochloride, salicylic acid, acetic acid, formic acid, sulfoacetic acid and glycolic acid. Stock solutions of the analytes in H₂O were prepared at 10 mM concentration of water soluble compounds and 5 mM for sparingly soluble compounds.

For low-field experiments, stock solutions of α -asarone were prepared at 300.0 mM concentration in 0.5 ml DMSO-d₆ and 2.0 ml deuterated methanol (MeOD). Naproxen tablets require prior preparation; they were crushed in a mortar and prepared to obtain *ca.* 10 mM concentration of naproxen in two samples: 100% DMSO-d₆ and a mixture of 20% DMSO-d₆ and 80% D₂O. According to the producer, each tablet (*ca.* 280 mg) contains 200 mg naproxen and excipients: 38.9 mg of lactose monohydrate and undeclared amounts of corn starch, magnesium stearate, polyvidone, colloidal silica, sodium dodecyl sulfate, and sunset yellow (E 110). All samples were shaken for 5 minutes on a vortex mixer, then the supernatant was collected for analysis (the precipitate contained probably only colloidal silica and some amount of starch).

2.2 NMR

The experiments to determine pK_a by Yasuda-Shedlovsky extrapolation were performed on a Bruker Avance III 500 MHz

spectrometer operating at 500.21 MHz for ¹H equipped with a Bruker SampleXpress sample changer that was used for repeated injection and reinsertion of samples (Fig. S6). Locking and shimming was performed on DMSO-d₆. The probe was equipped with z-axis pulsed field gradients. The temperature of the samples was maintained at 298 ± 0.5 K. The 90° pulse was 10 μs. The relaxation delay was 3 seconds. The spectral width was 20 ppm, and the number of data points were 32k, giving an acquisition time of 2.15 seconds. CSI experiments were performed using a gradient phase encoding sequence incorporating perfect echo excitation sculpting (ES) for water suppression.^{19,20} A spoil gradient (27 G cm⁻¹) was employed at the end of the signal acquisition period to destroy any transverse magnetization. The gradient pulse was 166 μs in duration and varied between -8 and 8 G cm⁻¹ in 32 steps. The shape of the pulse was a smoothed square. 4 ms Gaussian 180° pulses were employed for inverting magnetisation of the H₂O region. Four scans were acquired at each step giving a total acquisition time of 23 min. Sixteen dummy scans were acquired prior to signal acquisition. DSS was used as a chemical shift reference in all experiments (0 ppm). NMR data was processed in Bruker TopSpin 4.6.5 and Mnova 14.2.0 and CSI images were processed in phase sensitive mode following the procedure of Trigo-Mourino *et al.*¹⁹ Following two-dimensional Fourier transformation of the CSI data sets, the individual spectra were automatically extracted, any residual phase errors corrected, and the spectra referenced to DSS (0 ppm) using an automation script written in house.²⁰ Analyte and indicator chemical shift data were exported from TopSpin and Mnova into Microsoft Excel and subsequently analysed.

Experiments at low-field were performed on a Spinsolve Carbon 43 MHz benchtop spectrometer (Magritek GmbH, Germany). We used the SWAPE device²¹ to change the vertical position of the sample mechanically. All samples were measured at 16 different positions starting from 2 cm above the bottom of the NMR tube, and each successive value of the sample represents a step of 0.5 cm, while the active region of the RF coil is 1 cm. We performed ¹H NMR and ¹H-¹³C HSQC experiments for each volume of the asarone sample and ¹H NMR experiment for the naproxen sample. The experimental time for a single volume was 62 minutes for asarone and 4 minutes for naproxen. ¹H spectra were acquired with 8192 data points, giving an acquisition time of 1.64 seconds. The relaxation delay was 1.86 seconds, and 32 (asarone) or 64 (naproxen tablet) transients. The pulse length was 11.5 μs. Both ¹H and ¹H-¹³C HSQC experiment were set up using Spinsolve Expert software (version 2.01.19). The ¹H and ¹³C pulses were 61.1 μs. The non-uniform sampling (NUS) has been used (64 random points out of a full grid of 1024 increments). The NUS reconstruction was performed using a compressed sensing module of mddnmr software.²² The iteratively re-weighted least squares algorithm²³ has been used with 20 iterations and a virtual echo option.²⁴

2.3 Establishing solvent gradients for NMR analysis

To establish a solvent gradient spanning between 0.8 f_{DMSO} and 0.2 f_{DMSO} in a 5 mm NMR tube for analysis at high-field



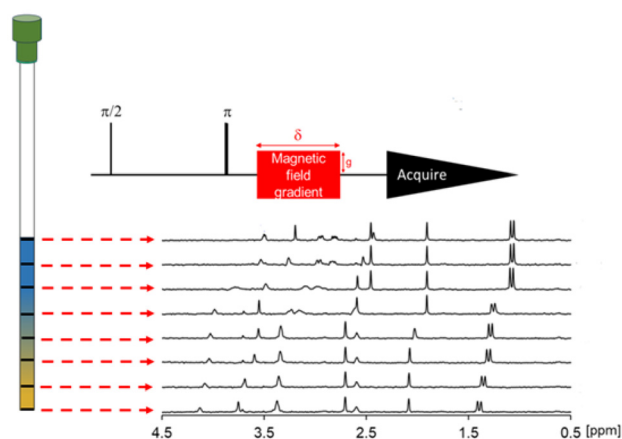


Fig. 1 Scheme of solvent gradient experiment. $0.2f_{\text{DMSO}}$ (blue) is layered on top of $0.8f_{\text{DMSO}}$. A gradient is formed, leading to changes in chemical shift when analysed by chemical shift imaging.

(Fig. 1), two solutions were prepared at both of these compositions containing the analyte, DSS, NaMSA, and the indicator/indicators. The concentration of the analyte was equal to the concentration of the indicator when one indicator was used. When multiple indicators were used (furosemide), the sum of their concentration equalled the concentration of the analyte (section S9). $320 \mu\text{l}$ of the $0.8f_{\text{DMSO}}$ solution was put into the NMR tube. This was followed by $320 \mu\text{l}$ of the $0.2f_{\text{DMSO}}$ solution being gently layered on top using a 9 inch Pasteur pipette. The $0.8f_{\text{DMSO}}$ solution was put at the bottom of the NMR tube due to it having a higher density. $2\text{D } ^1\text{H}$ chemical shift imaging experiments were then recorded on the sample. A smooth variation in solvent composition across the full range of compositions was obtained approximately 4 hours after preparation of the sample (see SI, section S8 for how that is determined). We note that a similar approach can be used to generate a smooth variation in the solvent composition between DMSO and chloroform (SI, section S12).

Samples for analysis at low-field were prepared using thin-walled NMR tubes 9" in length and 5 mm in outer diameter. The first step to establish a solvent gradient was to place a sample dissolved in DMSO- d_6 at the bottom of the NMR tube using a glass pipette (see Fig. 2). Then, we froze the sample in the refrigerator at a temperature of 6°C for about 15 minutes. Freezing the DMSO sample helps reduce solvent mixing during sample preparation. Then, we added a solution containing the studied substance and a second solvent – MeOD for asarone or a mixture of deuterium oxide and DMSO for naproxen tablet.

3 Results and discussion

3.1 Determination of $\text{p}K_{\text{a}}$ of analyte in pure water by Yasuda-Shedlovsky extrapolation

The Yasuda-Shedlovsky extrapolation equation is an empirical equation that linearly correlates the $\text{p}K_{\text{a}}$ of a compound in a

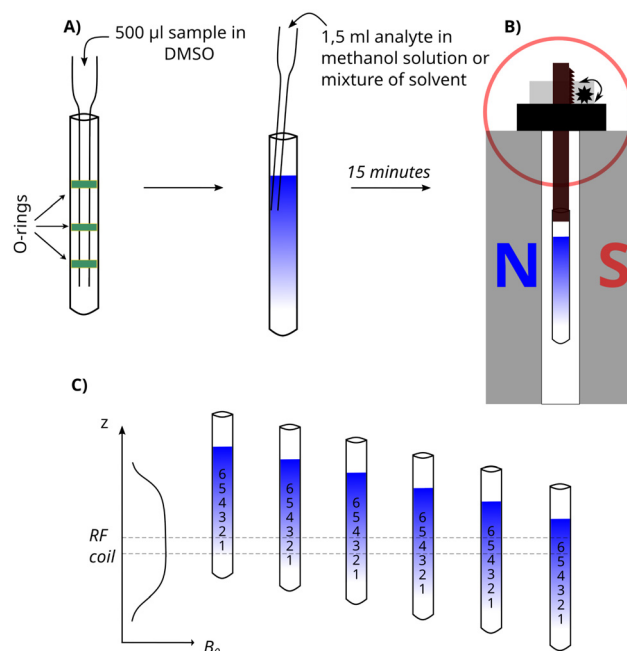


Fig. 2 Scheme of a solvent-gradient experiment using a 43 MHz BT-NMR. (A) General sample preparation procedure (the o-rings serve to guide the pipette down the centre of the sample tube). (B) Sample in SWAPE device (SWAPE motor marked in red) inside BT-NMR spectrometer. (C) The scheme of vertical sample shifting with respect to a B_0 field profile.

particular solvent composition with the dielectric constant (eqn (1)). It is a robust method for predicting the aqueous $\text{p}K_{\text{a}}$ values of water-insoluble system by extrapolating the $\text{p}K_{\text{a}}$ values in DMSO- d_6 /H $_2$ O mixtures to what the $\text{p}K_{\text{a}}$ would be in pure water.²⁵

$$\text{p}_s K_{\text{a}} + \log[\text{H}_2\text{O}]A/\varepsilon + B \quad (1)$$

Where $\text{p}_s K_{\text{a}}$ is the $\text{p}K_{\text{a}}$ of the compound at a specific solvent composition (SI, section S4), ε is the dielectric constant of the solvent and A and B are empirical constants. For that purpose, $\text{p}_s K_{\text{a}}$ of analyte, molar concentration of H $_2$ O, and dielectric constant of each 1D slice along the NMR tube need to be determined. H $_2$ O concentration was measured by determining the fraction of H $_2$ O present per slice and converting it to molar concentration (see SI, section S7). The dielectric constant was determined from the fractional volume of DMSO using the model of Jouyban *et al.* (see SI, section S5).²⁶ The fractional volume of DMSO was determined from the ^1H chemical shift of sodium methanesulfonate (NaMSA) which could be fitted to a third order polynomial (Fig. 3). The measurement of f_{DMSO} was unaffected by the presence of 5 mM HCl (SI section S6). We note that the ^1H chemical shifts of H $_2$ O and DMSO are not sufficiently sensitive to solvent composition below $0.5f_{\text{DMSO}}$ due to the non-ideality of DMSO–water mixtures.²⁷

The $\text{p}_s K_{\text{a}}$ of the acidic analyte is obtained by methods presented in our previous work.²⁸ In brief, $\text{p}_s K_{\text{a}}$ is determined by measuring the quantity of protons transferred (κ) to an indi-



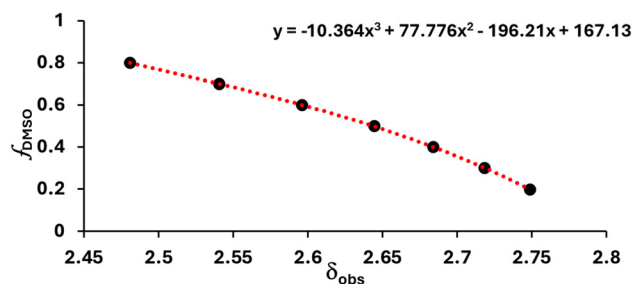


Fig. 3 Plot of f_{DMSO} versus δ_{obs} of NaMSA with respective fitting.

cator compound with a known p_sK_a and concentration. κ is related to the p_sK_a and concentration, C_{acid} , of the acidic analyte using eqn (2) (SI, section S1):

$$p_sK_a = \log\left(\frac{C_{\text{acid}}}{\kappa}\right) + \text{pH} \quad (2)$$

The pH of the solution throughout the different 1D spectra is determined using the indicator *via* the NMR modified Henderson–Hasselbalch equation:

$$\text{pH} = p_sK_a + \log\left(\frac{\delta_{\text{obs}} - \delta_{\text{H}}}{\delta_{\text{L}} - \delta_{\text{obs}}}\right) \quad (3)$$

where δ_{H} and δ_{L} are the limiting chemical shifts of the indicator when it is fully protonated and fully deprotonated, respectively (SI, section S2). The limiting chemical shifts and p_sK_a values of the indicators are experimentally determined at individual solvent compositions between 20% and 80% DMSO- d_6 and their values obtained across the whole compositional range by polynomial interpolation (see SI, section S3 and S11). pH and κ can thus be determined continuously across the compositional range between 20% and 80% DMSO- d_6 along the solvent gradient. The p_sK_a of the analyte can be determined across the different 1D slices, and subsequently the *A* and *B* parameters can be fitted by linear regression.

The method was initially validated on water-soluble compounds (see Fig. 4). Their pK_a values in pure water were determined using the method described within 0.4 units of literature (see Table 1). As discussed in our previous work, the uncertainty in pK_a , Δp_sK_a (section S10), increases with the difference between the pK_a of the analyte.²⁸ It is therefore desirable to use indicators that have pK_a values close to the expected values of the analyte. The proximity of pK_a values can be judged by comparison of inflexion points in plots of chemical shift *versus* pH.²⁸

We then analysed the poorly water-soluble compounds naproxen, furosemide, and indomethacin. Their behaviour was remarkably different compared to the water-soluble compounds. Fig. 5 shows how these compounds displayed a contrasting behaviour between DMSO-rich data and water-rich points. The two regimes could be represented as two lines, with better agreement with the values obtained from the literature pK_a by extrapolating from the DMSO-rich (see Table 1). Extrapolating from the water-rich data points (red lines, Fig. 5)

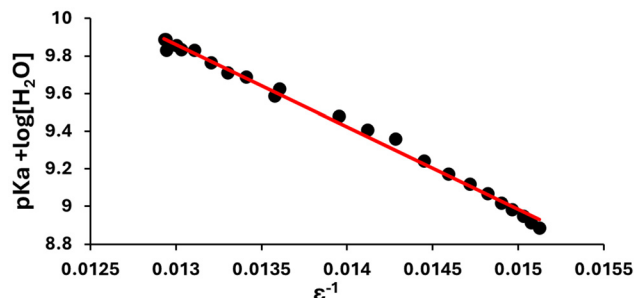
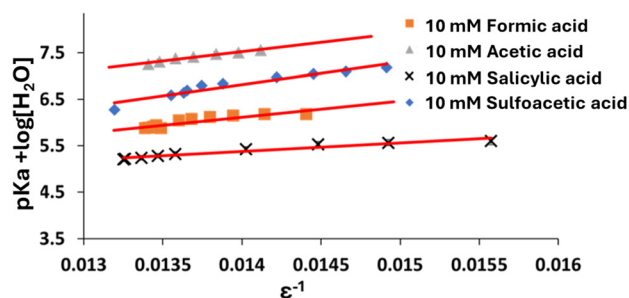


Fig. 4 Plot of $pK_a + \log[\text{H}_2\text{O}]$ versus $1/\epsilon$ of water soluble carboxylic acids (top) and quinine hydrochloride (bottom).

Table 1 Comparison of aqueous pK_a values of water soluble and sparingly soluble* compounds obtained *via* Yasuda–Shedlovsky extrapolation with literature values, with absolute difference, Δ

Analyte	Indicator	Literature pK_a	Fitted pK_a	ΔpK_a
Salicylic acid	1,2,4-Triazole	3.00 (ref. 29)	3.09	0.09
Formic acid	Sodium glycolate	3.75 (ref. 30)	3.92	0.17
Sulfoacetic acid	Sodium glycolate	4.07 (ref. 31)	4.37	0.30
Acetic acid	Sodium glycolate	4.77 (ref. 32)	5.16	0.39
Quinine hydrochloride	2-Methylimidazole	8.55 (ref. 33)	8.34	0.21
Naproxen*	Sodium formate	4.15 (ref. 34)	4.25	0.10
Indomethacin*	Sodium acetate	4.50 (ref. 35)	4.24	0.26
Furosemide*	Sodium formate, sodium glycolate	3.34 (ref. 36)	3.28	0.06

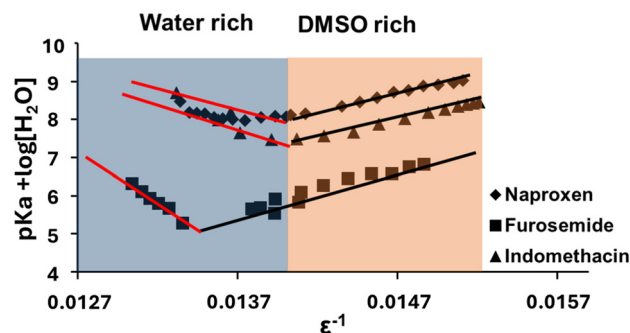


Fig. 5 Plot of $pK_a + \log[\text{H}_2\text{O}]$ versus $1/\epsilon$ of water insoluble analytes.



yields aqueous pK_a values of 7.0, 9.0 and 9.3 for furosemide, indomethacin and naproxen, respectively.

These results suggest aggregation or precipitation dynamics in the water-rich regime that are not present in the DMSO-rich one. Significant broadening of the naproxen, furosemide, and indomethacin resonances was observed in the water-rich region compared to the DMSO-rich region, (see Fig. 6), suggesting that aggregation was occurring. Aggregation is a major problem in pharmaceutical assays and NMR analysis.³⁷

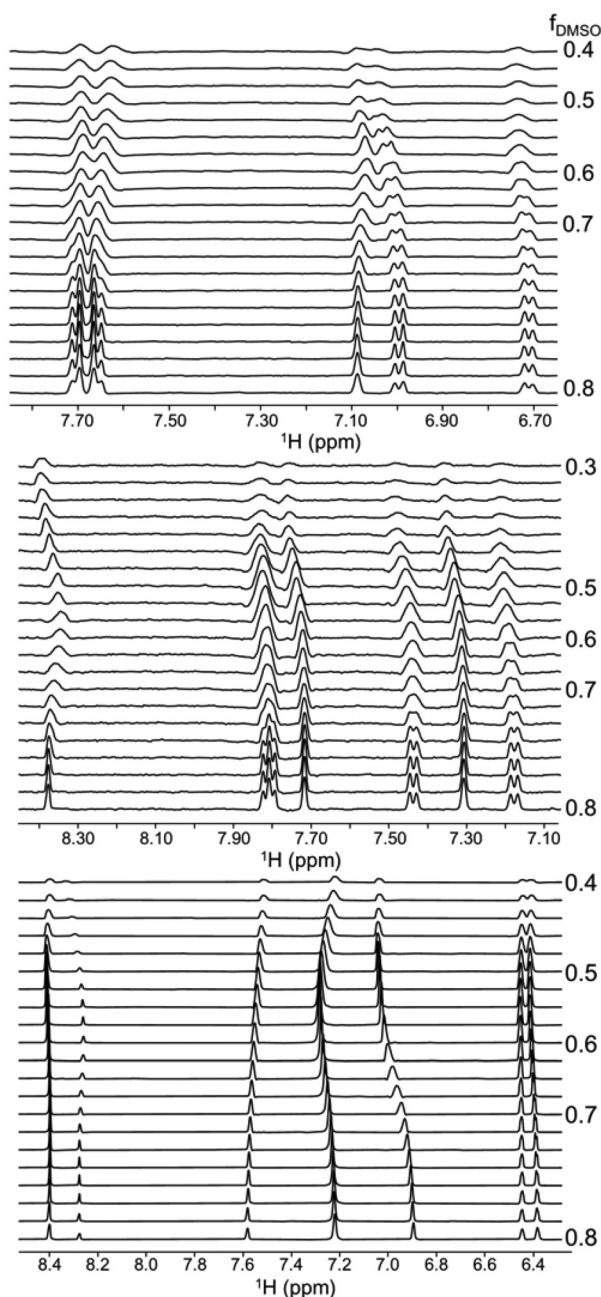


Fig. 6 Comparison of spectra of indomethacin (top); naproxen (middle) and furosemide (bottom) along solvent gradients at the fractional volume of DMSO indicated.

Our approach provides a fast method to determine the minimum quantity of DMSO required to keep drug molecules in the non-associated state by monitoring the acid–base properties of the molecules. Such features are readily apparent in the Yasuda-Shedlovsky plot due to the large number of pK_a values (>10) afforded by our method from a single experiment, highlighting a key advantage of our approach over separate pK_a determinations at homogeneous solvent compositions. Solvent gradients are usable at any time during a window between 4–8 hours after preparation (Fig. S6), enabling multiple compounds to be prepared during the daytime and analysed in parallel overnight under automation on spectrometers equipped with autosamplers.

We anticipate that the method could be applied to any aqueous–organic solvent mixture. The pK_a and limiting chemical shifts of the indicators would need to be determined at three or more individual solvent ratios. The parameters of a full set of indicators (pH 2–11) could be determined in just two CSI experiments for each solvent ratio if prior literature pK_a values were available to anchor the pH scales.²⁰ Calibration of an absolute reference could be performed in an additional two CSI experiments, or alternatively the parameters of the indicators could be determined using automated NMR titrations.³⁸ Calibration of a suitable indicator of the solvent composition such as methanesulfonate would also be required.

3.2 Transferring assignment between samples in different solvents

The solvent typically affects chemical shifts, resulting in significant changes to the peak pattern of an NMR spectrum.³⁹ Advanced computational methods can model them only in relatively simple cases.⁴⁰ Because of this, resonance assignments performed in one solvent cannot be simply transferred to spectra acquired in a different solvent, necessitating the repetition of a laborious assignment procedure. In such cases, solvent-gradient experiments can be helpful.

Fig. 7 (upper panel) shows a ^1H NMR spectrum of α -asarone acquired at 43 MHz. As can be seen, the signals from methyl groups strongly overlap, and their assignment requires time-consuming heteronuclear 2D experiments. Once the assignment is achieved in one solvent, it would be very unfavorable to repeat it in another, especially taking into account the low sensitivity of benchtop NMR. Fortunately, the solvent-gradient experiment reveals a smooth trajectory of chemical shifts, enabling the transfer of assignments. Fig. 7 (lower panel) shows superimposed fragments of fifteen 2D ^1H - ^{13}C HSQC spectra acquired in a DMSO:MeOD gradient. Clearly, the peak patterns differ in pure solvents, which may make the transfer ambiguous. However, with spectra acquired in a gradient, the transfer trajectories become clear.

3.3 Resolving the spectrum of a mixture

The various components of a solid-state mixture, such as a drug tablet, may exhibit different solubilities in a given solvent. This effect can be used to resolve ambiguities in the



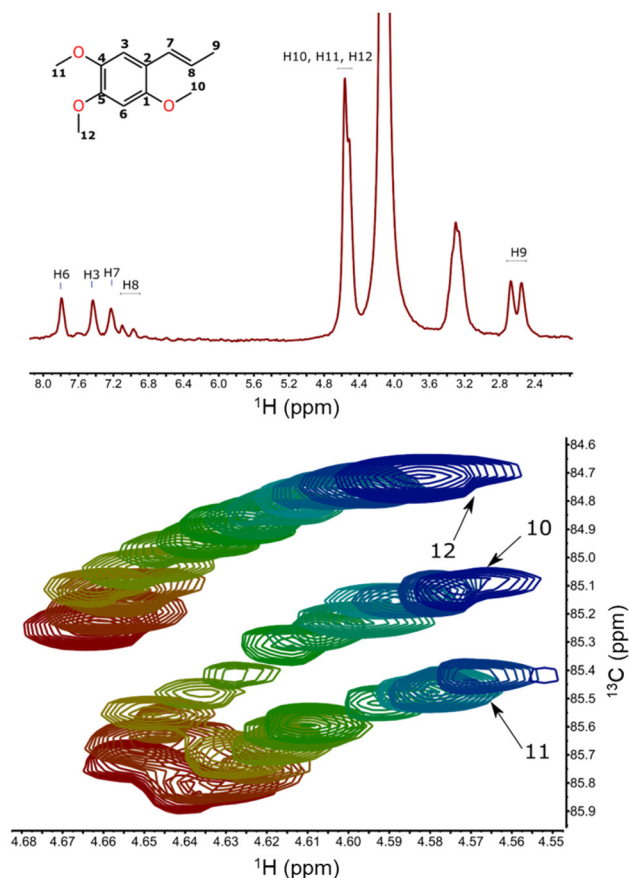


Fig. 7 NMR spectra of α -asarone in MeOD measured on a 43 MHz benchtop NMR: ^1H NMR (upper panel) and a stack of fifteen 2D ^1H - ^{13}C HSQC spectra measured in solvent gradient DMSO : MeOD in methoxy group region. The experiments were performed 5 days after sample preparation (red corresponds to DMSO, blue – MeOD, other to mixtures).

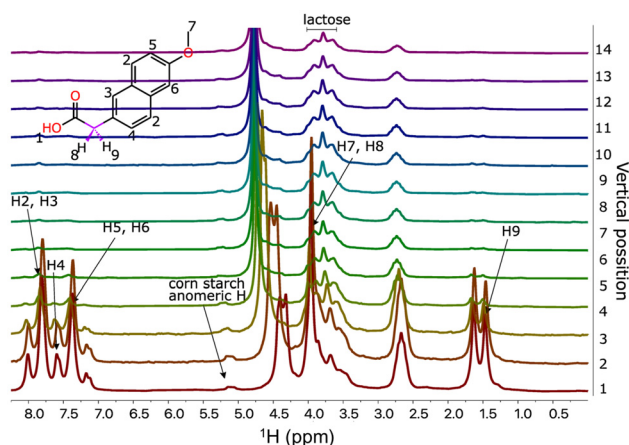


Fig. 8 Stack of ^1H NMR spectra of naproxen drug (200 mg naproxen in a tablet, Aflofarm Farmacja Polska Sp. z o.o.) measured on 43 MHz benchtop NMR in solvent gradient DMSO : 80% D_2O : 20% DMSO. The experiments were performed 24 h after sample preparation (red (first one down) corresponds to DMSO, pink (last one at the top) – 80% D_2O : 20% DMSO, other to mixtures).

spectra of mixtures and is especially useful for low-field machines.

Fig. 8 shows the set of spectra of naproxen drug tablet dissolved in a gradient of D_2O and DMSO. The DMSO is an effective solvent for all main ingredients – naproxen, lactose, and starch – and thus the spectrum is very crowded. The peak overlap makes the identification of resonances impossible. However, the gradient of solvent composition creates a spectral “pseudo-dimension” that resolves peaks based on the solubility of a given component. It also allows for the identification of which peaks probably belong to the same compound, since they have to follow the same intensity change along the gradient.

4 Conclusions

We have demonstrated how the solvent composition across an NMR sample can be varied from DMSO to water, and DMSO to methanol *via* the diffusion of two layers of solvent. This procedure condenses tedious manual titrations and enables the measurement of key properties including pK_a values, chemical shifts and 2D correlations as a continuous function of the solvent composition in one sample. Our methods can be applied both to solutions and to semi-solid samples (naproxen tablet), promising a range of future applications from materials science to pharmaceutical analysis and organic synthesis; all areas where control and optimisation of the solvent is vital.

Author contributions

Conceptualization: H. H., M. W., K. K., P. P.; data curation: all authors; formal analysis: H. H., M. W., K. K., P. P.; funding acquisition: M. W., K. K.; investigation, validation, and methodology: all authors; project administration and supervision: M. W., K. K.; resources: M. W., K. K.; visualization: H. H., P. P.; writing – original draft: H. H., M. W., K. K., P. P.; writing – review & editing: all authors.

Conflicts of interest

There are no conflicts to declare.

Data availability

Additional data supporting this article are available in the supplementary information (SI). Research data will be available at: <https://research-portal.uea.ac.uk/en/datasets/>. The pulse sequences and processing scripts are freely available on the UEA Digital Repository (<https://research-portal.uea.ac.uk/en/datasets/data-for-measurement-of-the-pka-values-of-organic-molecules-in-aq/>) in conjunction with our prior published work.



Supplementary information: experimental and calculation procedures, plots for NMR indicators. See DOI: <https://doi.org/10.1039/d6an00031b>.

Acknowledgements

The work was supported by the Polish National Science Centre grant no. 2019/35/B/ST4/01506, UKRI Future Leaders Fellowship (MR/T044020/1 and MR/Z000114/1) to MW and UEA Faculty of Science PhD studentship to HH. We are grateful for the use of the University of East Anglia Faculty of Science NMR facility.

References

- M. Orozco and F. J. Luque, *Chem. Rev.*, 2000, **100**, 4187–4226.
- C. Reichardt, *Org. Process Res. Dev.*, 2007, **11**, 105–113.
- M. Hein, S. Arena and C. Willard, *Foundations of college chemistry*, John Wiley & Sons, 2016, pp. 313–314.
- T. Chan, I. Lee and K. Chan, *J. Phys. Chem. B*, 2014, **118**, 10945–10955.
- U. Kappas, W. Fischer, E. Polymeropoulos and J. Brickmann, *J. Theor. Biol.*, 1985, **112**, 459–464.
- M. H. Abraham, *Pure Appl. Chem.*, 1985, **57**, 1055–1064.
- F. L. Mota, A. P. Carneiro, A. J. Queimada, S. P. Pinho and E. A. Macedo, *Eur. J. Pharm. Sci.*, 2009, **37**, 499–507.
- A. J. Parker, *Chem. Rev.*, 1969, **69**, 1–32.
- M. F. J. Mabesoone, A. R. A. Palmans and E. W. Meijer, *J. Am. Chem. Soc.*, 2020, **142**, 19781–19798.
- B. Gutbezahl and E. Grunwald, *J. Am. Chem. Soc.*, 1953, **75**, 559–565.
- J. T. Hynes, *J. Stat. Phys.*, 1986, **42**, 149–168.
- G. Castro, O. Giordano and S. Blanco, *J. Mol. Struct.: THEOCHEM*, 2003, **626**, 167–178.
- R. Molina-Muriel, J. R. Romero, Y. Li, G. Aragay and P. Ballester, *Org. Biomol. Chem.*, 2021, **19**, 9986–9995.
- P. Mukerjee and J. D. Ostrow, *BMC Biochem.*, 2010, **11**, 1–12.
- S. Boobier, Y. Liu, K. Sharma, D. R. Hose, A. J. Blacker, N. Kapur and B. N. Nguyen, *J. Chem. Inf. Model.*, 2021, **61**, 4890–4899.
- J. Hernández-Lima, K. Ramírez-Gualito, B. Quiroz-García, A. L. Silva-Portillo, E. Carrillo-Nava and F. Cortés-Guzmán, *Front. Chem.*, 2022, **10**, 1012769.
- P. P. Madeira, J. A. Loureiro, M. G. Freire and J. A. Coutinho, *J. Mol. Liq.*, 2019, **274**, 740–745.
- G. F. Pauli, U. Kuczkowiak and A. Nahrstedt, *Magn. Reson. Chem.*, 1999, **37**, 827–836.
- P. Trigo-Mouriño, C. Merle, M. R. Koos, B. Luy and R. R. Gil, *Chem. – Eur. J.*, 2013, **19**, 7013–7019.
- M. Wallace, N. Abiama and M. Chipembere, *Anal. Chem.*, 2023, **95**, 15628–15635.
- J. A. Romero, K. Kazimierczuk and D. Gołowicz, *Analyst*, 2020, **145**, 7406–7411.
- V. Y. Orekhov, V. Jaravine, M. Mayzel and K. Kazimierczuk, *mddnmr.spektrino.com*, 2004–2024.
- K. Kazimierczuk and V. Orekhov, *Angew. Chem., Int. Ed.*, 2011, **50**, 5556–5559.
- M. Mayzel, K. Kazimierczuk and V. Orekhov, *Chem. Commun.*, 2014, **50**, 8947–8950.
- K. Takács-Novák, K. J. Box and A. Avdeef, *Int. J. Pharm.*, 1997, **151**, 235–248.
- A. Jouyban, S. Soltanpour and H.-K. Chan, *Int. J. Pharm.*, 2004, **269**, 353–360.
- K. Mizuno, S. Imafuji, T. Ochi, T. Ohta and S. Maeda, *J. Phys. Chem. B*, 2000, **104**, 11001–11005.
- H. Hussain, Y. Z. Khimyak and M. Wallace, *Anal. Chem.*, 2024, **96**, 19858–19862.
- R. SalinasáMayorga, *et al.*, *J. Chem. Soc., Faraday Trans.*, 1992, **88**, 3025–3032.
- J. Mollin, Z. Pavelek, J. Navrátilová and A. Recmanová, *Collect. Czech. Chem. Commun.*, 1985, **50**, 2670–2678.
- C. V. Banks and J. Zimmerman, *J. Org. Chem.*, 1956, **21**, 1439–1440.
- A. J. Hoefnagel and B. M. Wepster, *Recl. Trav. Chim. Pays-Bas*, 1990, **109**, 455–462.
- L. Settimo, K. Bellman and R. M. Knegetel, *Pharm. Res.*, 2014, **31**, 1082–1095.
- P. Bustamante, M. A. Peña and J. Barra, *J. Pharm. Pharmacol.*, 1998, **50**, 975–982.
- M. O'Brien, J. McCauley and E. Cohen, *Indomethacin*, Academic Press, 1984, vol. 13, pp. 211–238.
- S. Winiwarter, N. M. Bonham, F. Ax, A. Hallberg, H. Lennernäs and A. Karlén, *J. Med. Chem.*, 1998, **41**, 4939–4949.
- S. R. LaPlante, R. Carson, J. Gillard, N. Aubry, R. Coulombe, S. Bordeleau, P. Bonneau, M. Little, J. O'Meara and P. L. Beaulieu, *J. Med. Chem.*, 2013, **56**, 5142–5150.
- E. N. A. Sundén, S. Karlsson, C. Bauer and P.-O. Norrby, *React. Chem. Eng.*, 2026, **11**, 359–366.
- M. Rytel, P. Kasprzak, P. Setny and K. Kazimierczuk, *Phys. Chem. Chem. Phys.*, 2019, **21**, 19209–19215.
- M. Dračinský and P. Bouř, *J. Chem. Theory Comput.*, 2010, **6**, 288–299.

